Proceedings of the 1999 IEEE/ASME
International Conference on Advanced Intelligent Mechatronics
September 19-23, 1999 • Atlanta, USA

H_∞ Yaw-Moment Control with Brakes for Improving Driving Performance and Stability

Jong Hyeon Park and Woo Sung Ahn

Hanyang University
School of Mechanical Engineering
17 Sungdong-ku, Haengdang-dong, Seoul, 133-791, Korea
jongpark@email.hanyang.ac.kr

Abstract— **This paper proposes a new H_∞ yaw-moment control scheme using brake torque for improving vehicle performance and stability especially in high speed driving. Its characteristics is that only one brake is used for control depending on the vehicle state. Steering angles are modeled as a disturbance input to the system and the controller minimizes the difference between the performance of the actual vehicle behavior and that of its 'model' behavior under the disturbance input. Various simulations with a nonlinear 8-DOF vehicle model show that the controller enhances the vehicle performance and stability.**

Keywords— **H_∞ Control, Yaw Moment Control, Yaw Rate, Vehicle Stability, Side Slip Angle, Switching Control Scheme.**

I. INTRODUCTION

Safety of vehicles has been improved considerably in recent years. Vehicle stability is achieved by various passive and active safety devices. Air-bags and seat belt tensioners are typical passive equipment to minimize damages in vehicle accidents. By contrast, active safety systems are to prevent accidents before they occur. More and more automobiles adopt some kind of active safety systems. They include ABS (antilock brake system), TCS (traction control system), and 4WS (4-wheel steering) system.

Since the beginning of 1980s, 4WS (4-wheel steering) systems have been regarded as being effective in improving vehicle performance and stability. Various active control systems for 4WS have been developed and commercially marketed. However, it is associated with high vehicle tag price due to its separate actuators for the rear steering, and high maintenance cost. Now the market for the 4WS is significantly shrunk despite its technical excellence in enhancing the stability and performance of vehicles.

As an alternative to 4WS systems, yaw moment control systems have been researched and developed. Yaw moment control directly generates the right amount of yaw moment for a vehicle to have good handling performance and stability. The yaw moment can be produced by actively increasing tractive force transmitted through the power train, or by applying braking forces at the wheels.

Some researchers have emphasized only the development of the control logic of yaw moment control cooperated with 4WS ignoring how the yaw moment is generated [1, 2]. Other researchers proposed PID controls or LQ-optimal controls to compensate the error between the actual state and desired state of the vehicle [3, 4, 5]. And many studies have been done about controlling vehicle slip ratio to generate sufficient lateral forces and longitudinal forces [3, 6]. However, most of them do not guarantee the robustness to uncertainty in vehicle parameters and disturbances that are intrinsically associated with vehicles. In actual driving, the conditions of the vehicle and the road that it rides on continuously change. In order to be used in actual driving conditions, any active control system of vehicles should have enough performance and stability robustness.

This paper proposes a design method based upon an H_∞ optimal yaw-moment control for controlling brake torque. This method assures the robust stability and robust performance to the changes in the system parameters and disturbances. The H_∞ controller is obtained based on a 2-DOF linear vehicle model, which represents the lateral and yaw motions of a vehicle. The controller is designed to follow a model behavior which depends on the steering angle. Driving a front-wheel-driven vehicle with the designed controller is simulated. The vehicle model used in simulation is nonlinear and has 8-DOF including the dynamics of its brake actuators. For the simulations, Dugoff nonlinear tire model is used, which is good in simulating the situations when steering and braking occur simultaneously.

In section II, the vehicle dynamics of lateral and yaw

0-7803-5038-3/99/$10.00 © 1999 IEEE

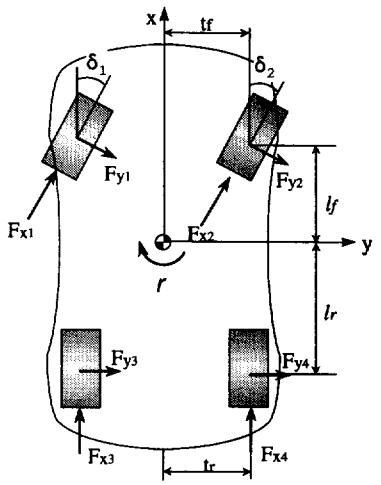

Fig. 1. A front-wheel-driven vehicle model and its related forces.

motions is described. Control logic and the design of H_∞ controller with its μ-analysis for robust stability and performance are presented in section III. Section IV describes vehicle simulations and their results, followed by conclusions in section V.

II. VEHICLE DYNAMICS

The basic vehicle model used for the later simulations is a 8-DOF model. Based on the coordinate frames shown in Fig. 1, the dynamic equations of the vehicle can be obtained as

$$M(\dot{V}_x - V_y r) = F_{x1}\cos\delta_1 + F_{x2}\cos\delta_2 - F_{y1}\sin\delta_1 - F_{y2}\sin\delta_2 + F_{x3} + F_{x4}, \quad (1)$$

$$M(\dot{V}_y + V_x r) = F_{x1}\sin\delta_1 + F_{x2}\sin\delta_2 + F_{y1}\cos\delta_1 + F_{y2}\cos\delta_2 + F_{y3} + F_{y4}, \quad (2)$$

$$\begin{aligned} I_z\dot{r} = {} & t_f(F_{x1}\cos\delta_1 - F_{x2}\cos\delta_2 - F_{y1}\sin\delta_1 + F_{y2}\sin\delta_2) \\ & + t_r(F_{x3} - F_{x4}) \\ & + l_f(F_{x1}\sin\delta_1 + F_{x2}\sin\delta_2 + F_{y1}\cos\delta_1 + F_{y2}\cos\delta_2) \\ & - l_r(F_{y3} + F_{y4}) \end{aligned} \quad (3)$$

where F_x and F_y denote the longitudinal force and the lateral force generated by the tires, respectively; V_x, V_y, and r denote the longitudinal velocity, the lateral velocity, and yaw rate, respectively; M and I_z denote the mass of the vehicle and the yaw moment of inertia about its mass center; and δ_i denotes the steering angle at wheel i.

Assuming that a front-wheel-driven vehicle is modeled, its wheel slip angles are expressed by

$$\begin{aligned} \alpha_1 &= \delta_1 - \tan^{-1}\left(\frac{V_y + l_f r}{V_x + t_f r}\right), \\ \alpha_2 &= \delta_2 - \tan^{-1}\left(\frac{V_y + l_f r}{V_x - t_f r}\right), \\ \alpha_3 &= -\tan^{-1}\left(\frac{V_y - l_r r}{V_x + t_r r}\right), \\ \alpha_4 &= -\tan^{-1}\left(\frac{V_y - l_r r}{V_x - t_r r}\right) \end{aligned} \quad (4)$$

where l_f and l_r are the distances from the center of mass to the front and rear axles, respectively; and t_f and t_r are the halves of the front and rear treads, respectively.

And, the side slip angle, β, is defined as the angle between the longitudinal axis of the vehicle and the its local velocity at the center, and thus

$$\beta = \tan^{-1}(V_y/V_x). \quad (5)$$

The tire forces, F_x and F_y are described as nonlinear functions of the slip ratio, the slip angle, the normal forces and the velocity of the tires. Here, the Dugoff model [7] is used to simulate the tire characteristics. The key parameters of the vehicle and the tire are summarized in Table I.

TABLE I

PARAMETERS OF THE VEHICLE AND THE TIRES USED IN THE PAPER.

Parameter		Value	Unit
M	vehicle mass	1,600	kg
I_z	vehicle yaw inertia	460	kgm^2
t_f	a half of front tread	0.761	m
t_r	a half of rear tread	0.755	m
C_l	tire longitudinal stiffness	52,526	N/unit slip
C_α	tire cornering stiffness	29,000	N/rad
h	height of the mass center	0.52	m
k_r	roll stiffness	69.82	kNm/rad
b_r	roll damping coeff.	3,512	Nms/rad

III. CONTROLLER DESIGN

A. Simplified Dynamics

In this section, a simplified vehicle dynamics that will be used in the controller design is derived. Since the vehicle dynamics in the lateral and yaw directions plays an important role, especially during high-speed cornering maneuver, the simplified dynamics in these directions are first considered here.

First, under the assumption that $V_x \gg V_y$, Eq. (5) results in

$$\beta \approx V_y/V_x. \tag{6}$$

It is also assumed that the steering angles are small, i.e., $\delta_1 \approx \delta_2 = \delta_f \ll 1$, and that the front and rear treads are approximately equal, i.e.,

$$t_r \approx t_f = t.$$

Also, considering that Eq. (4) can be simplified under the assumption of $V_x \gg t_f r$, and $V_x \gg t_r r$, Eqs. (2)–(4) can be simplified as

$$M(\dot{V}_y + V_x r) = \sum_{i=1}^{2} F_{xi}\delta_i + \sum_{i=1}^{4} F_{yi} \tag{7}$$

$$\begin{aligned} I_z\dot{r} = {} & t(F_{x1} - F_{x2} - F_{y1}\delta_f + F_{y2}\delta_f + F_{x3} - F_{x4}) \\ & + l_f(F_{x1}\delta_f + F_{x2}\delta_f + F_{y1} + F_{y2}) \\ & - l_r(F_{y3} + F_{y4}) \end{aligned} \tag{8}$$

$$\begin{aligned} \alpha_{1,2} &= \delta_f - \tan^{-1}\left(\frac{V_y + l_f r}{V_x}\right), \\ \alpha_{3,4} &= -\tan^{-1}\left(\frac{V_y - l_r r}{V_x}\right). \end{aligned} \tag{9}$$

It is also assumed that the lateral force at a tire is linear with respect to its wheel slip angle, i.e.,

$$F_{yi} = C_{\alpha i}\alpha_i \quad i = 1, \ldots, 4, \tag{10}$$

where $C_{\alpha i}$ is the cornering stiffness of tire i.

Also, assuming a quasi-static moment balance at the wheels about their rotational centers,

$$F_{xi} = T_{bi}/R_w \tag{11}$$

where R_w is the effective wheel radius and T_{bi} is the braking torque at tire i.

Using Eq. (6)–(11), a state-space representation of a simplified vehicle model in the lateral and yaw directions is obtained as

$$\begin{bmatrix}\dot{\beta}\\ \dot{r}\end{bmatrix} = \begin{bmatrix}a_{11} & a_{12}\\ a_{21} & a_{22}\end{bmatrix}\begin{bmatrix}\beta\\ r\end{bmatrix} + \begin{bmatrix}0 & 0 & 0 & 0\\ b_{21} & b_{22} & b_{23} & b_{24}\end{bmatrix}\begin{bmatrix}T_{b1}\\ T_{b2}\\ T_{b3}\\ T_{b4}\end{bmatrix} + \begin{bmatrix}c_1\\ c_2\end{bmatrix}\delta_f \tag{12}$$

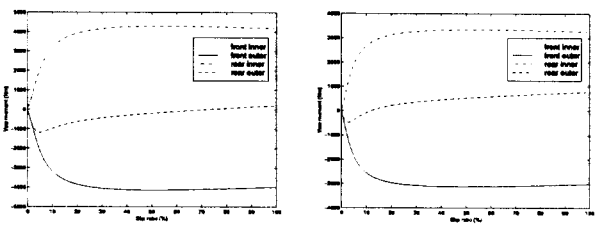

(a) (b)

Fig. 2. Yaw moment vs. slip angle depending on where brake torque is applied during steady cornering on (a) a dry road and (b) a slippery road.

where

$$a_{11} = -\frac{C_{\alpha f} + C_{\alpha r}}{MV_x}, \qquad a_{12} = -1 + \frac{C_{\alpha r}l_r - C_{\alpha f}l_f}{MV_x^2},$$

$$a_{21} = \frac{C_{\alpha r}l_r - C_{\alpha f}l_f}{I_z}, \qquad a_{22} = -\frac{C_{\alpha r}l_r^2 + C_{\alpha f}l_f^2}{I_z V_x},$$

$$b_{21} = b_{23} = -\frac{t}{I_z R_w}, \qquad b_{22} = b_{24} = \frac{t}{I_z R_w},$$

$$c_1 = \frac{C_{\alpha f}}{MV_x}, \qquad c_2 = \frac{C_{\alpha f}l_f}{I_z}.$$

B. Switching Control Scheme

Desired yaw moment can be generated by applying brake torque to the wheels. However, all wheels are not equally effective in generating the yaw moment. Brake torque applied at particular wheel may be more effective than the others in generating the required yaw moment. And, the effectiveness in generating yaw moment at one wheel changes depending on its operating conditions.

In order to determine the most effective wheel in generating yaw moment, a series of computer simulations were done for steady-state turns at various road conditions, i.e., with different values of road friction coefficients. At a steady state, a predetermined amount of brake torque was applied at one wheel at a time. As seen in Fig. 2 (a), a significant oversteer correction can be obtained by applying the brake torque at the front-outer wheel. Similarly, a significant understeer correction is obtained by applying the brake torque at the rear-inner wheel, regardless of the slip ratio, as seen in Fig. 2 (b). Based on this observation, a new scheme of switching the control inputs is suggested and implemented.

In order for the control system to achieve a consistent vehicle behavior no matter what the vehicle driving condition is, it is desirable to apply the brake torque at the most effective and consistent wheel. The proposed control scheme is to apply brake torque only at the wheel that is the most effective in generating yaw moment: the front-outer or the rear inner wheel.

When some understeer correction is required, brake torque is applied at the rear-inner wheel, and when some oversteer correction is required, brake torque is applied at the front-outer wheel.

Another advantage of applying the brake torque only at one wheel at a time is that brake torque at one wheel decelerates the vehicle less than brake torque at two or more wheels with the same amount of yaw moment generated. This characteristics is valuable especially in high speed driving.

When brake torque is applied only at a wheel, Eq. (12) becomes

$$\begin{bmatrix}\dot{\beta}\\ \dot{r}\end{bmatrix} = \begin{bmatrix}a_{11} & a_{12}\\ a_{21} & a_{22}\end{bmatrix}\begin{bmatrix}\beta\\ r\end{bmatrix} + \begin{bmatrix}c_1\\ c_2\end{bmatrix}\delta_f + \begin{bmatrix}0\\ b_{2i}\end{bmatrix}T_{bi} \quad (13)$$

where i =1, 2, 3, or 4. The index i is selected according to following control logic. When the desired yaw rate is smaller than the measured yaw rate, i is 1 or 2 during turning to the right and left, respectively. And, when the desired yaw rate is larger than the measured yaw rate, i is 3 or 4 during turning to the left and right, respectively.

Before determining the desired vehicle behavior, let's take Laplace transforms to both sides of Eq. (13). After simple algebraic manipulations of transfer functions,

$$r(s) = G_r(s)\delta_f + G_p(s)T_{bi} \quad (14)$$

where

$$G_r(s) = \frac{c_2 s + c_1 a_{21} - c_2 a_{11}}{s^2 - (a_{22}+a_{11})s + a_{11}a_{22} - a_{12}a_{21}}$$

$$G_p(s) = \frac{b_{2i}(s - a_{11})}{s^2 - (a_{22}+a_{11})s + a_{11}a_{22} - a_{12}a_{21}}.$$

Now, the model to generate the desired behavior characteristics of the vehicle is to be obtained. The desired yaw rate response to an steering-wheel angular input is assumed to be represented by a first-order system. The DC gain of the model is selected to be equal to the DC gain of the vehicle when no controller is used. This would give the driver an identical feeling during steady cornering whether the controller is used or not. The desired side slip angle is selected to be zero all the time. Thus, the desired vehicle model is

$$x_d(s) = \begin{bmatrix}\beta_d(s)\\ r_d(s)\end{bmatrix} = \begin{bmatrix}0\\ K_r/(1+\tau_r s)\end{bmatrix}\delta_f \quad (15)$$

where $K_r = G_r(0) = (c_1 a_{21} - c_2 a_{11})/(a_{11}a_{22} - a_{12}a_{21})$.

C. H_∞ Controller Design

Equation (13) can be represented state-space form of

$$\dot{x} = Ax + Bu + C\delta_f \quad (16)$$

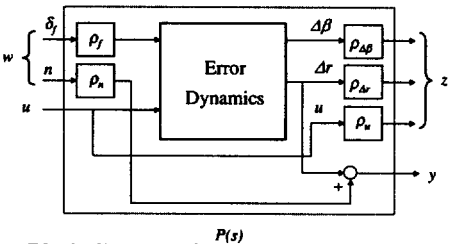

Fig. 3. Block diagram of the augmented error dynamics.

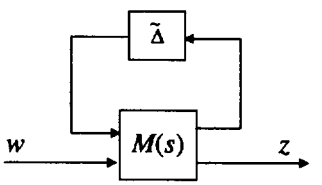

Fig. 4. Block diagram for performance robustness.

where $x = [\beta \quad r]^T$ and $u = T_{bi}$. And, Eq. (15) is also represented in the state-space form of

$$\dot{x}_d = A_d x_d + C_d \delta_f. \quad (17)$$

From Eqs. (16) and (17), the error dynamics becomes

$$\dot{e} = \tilde{A}e + Hu + \tilde{C}\delta_f \quad (18)$$

where $e := [\beta_d - \beta \quad r_d - r]^T$, $\tilde{A} = A_d - A$, $\tilde{C} = C_d - C$, and $H = -B$.

In order to formulate the standard structure for the H_∞ controller design, the error dynamics model is transformed into the one shown in Fig. 3, where w consists of the steering angle and the measurement noise, performance variable z consists of the side slip angle error, $\Delta\beta$, the yaw rate error, Δr, and the control effort, u. The weighting factors are selected to be $\rho_{\Delta\beta} = 0.6667$, $\rho_{\Delta r} = 0.7143$, $\rho_f = 0.0525$, $\rho_n = 0.001$, and $\rho_u = 0.0001$. Output y is the difference between the desired yaw rate and the measured yaw rate.

The augmented system in Fig. 3 can be expressed by

$$\begin{aligned}\dot{x_a} &= A_1 x_a + B_1 w + B_2 u\\ z &= C_1 x_a + D_{11} w + D_{12} u\\ y &= C_2 x_a + D_{21} w + D_{22} u\end{aligned} \quad (19)$$

where $x_a = e \in \mathbb{R}^2$, $w \in \mathbb{R}^2$, and $u, y \in \mathbb{R}^1$.

Note that only the measured yaw rate is fed back, and that $D_{11} = 0$ and $D_{22} = 0$. Since that (A_1, B_2, C_2) is stabilizable and detectable, and that both systems (A_1, B_2, C_1, D_{12}) and (A_1, B_1, C_2, D_{21}) have no transmission zeros in $j\omega$-axis, it is possible to find a stabilizing controller $K(s)$ without any mapping. The optimal controller that satisfies $||T_{zw}||_\infty < \gamma$, where $T_{zw}(s)$ is

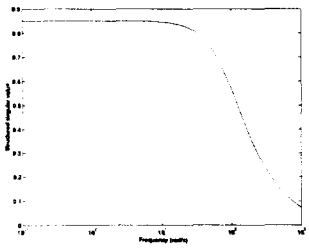

Fig. 5. μ-plot.

the transformation matrix from w to z, can be obtained by solving two algebraic Riccati equations [8, 9].

The optimal value for the current system was found to be 0.146, but a sub-optimal controller corresponding to $\gamma = 0.195$ is used instead in order to increase its robustness.

D. μ-Analysis

Since that the vehicle dynamics is intrinsically nonlinear and that its parameters change often, a stabilizing controller should be robust to model uncertainty.

It is considered that the mass of the vehicle and the cornering stiffness of the tire change as much as $\pm$ 30% and $\pm$ 50%, respectively. To assess the robust performance of the closed loop system, let's define an augmented perturbation structure, $\tilde{\Delta}$,

$$\tilde{\Delta} := \begin{bmatrix} \Delta & 0 \\ 0 & \Delta_p \end{bmatrix}$$

where Δ is parametric uncertainty block, Δ_p is the imaginary performance perturbation block. Both Δ and Δ_p are norm-bounded. From the μ-analysis theorem [9], the stability and performance robustness of the system is assured if and only if $M(s)$, shown in Fig. 4, is stable and

$$\max \mu_{\tilde{\Delta}}(M(j\omega)) < 1.$$

where $M(s)$ is the transfer function matrix including controller.

Figure 5 shows that the μ plot of the H_∞ control whose peak value is smaller than 1. Hence proposed H_∞ controller can achieve the robust performance and robust stability.

IV. SIMULATIONS

For the validation of the proposed robust control system, simulations are carried out under various conditions. For all simulations, brake actuator dynamics, represented by first-order plants, were included in the simulation model of the vehicle. Throughout the simulations, the vehicle was driven at 72 km/h.

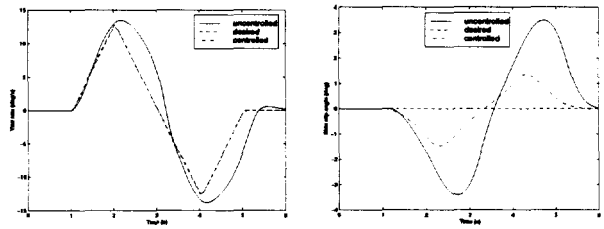

Fig. 6. (a) Yaw rate and (b) side slip angle during a lane change on a slippery road.

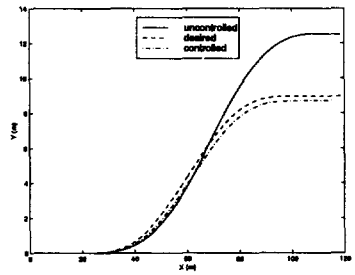

Fig. 7. Vehicle trajectory during a lane change on a slippery road.

In the first simulation, the vehicle changed its driving lanes on a slippery low μ road. The yaw rate, the side slip angle, the trajectory of the vehicle are shown in in Figs. 6 (a) and (b), and 7, respectively. Figure 6 shows that the vehicle with the H_∞ controller exhibits a better performance than that of the uncontrolled vehicle. Note that the yaw rate responses of the desired model and the controlled vehicle look almost identical in Fig. 6 (a). And, it can be observed in Fig. 7 that the controlled vehicle follows much closely to the desired trajectory. Control inputs shown in Fig. 8 indicates that there were switchings in the wheels where brake torque was applied.

In the second simulation, the vehicle made a J-turn motion. It was under the condition that the mass of the vehicle was increased by 30%. The yaw rate and the side slip angle are shown in Fig. 9. Also, note that the yaw rates of the desired model and the controlled

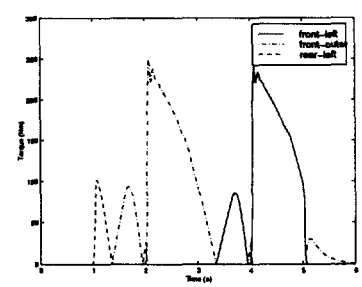

Fig. 8. Brake torque during a lane change on a slippery road.

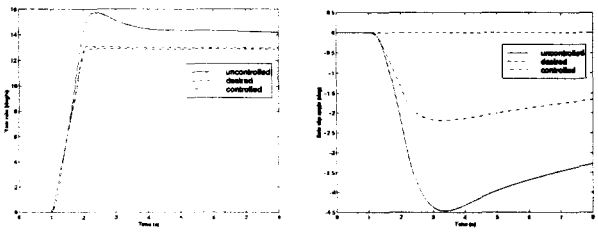

(a) (b)

Fig. 9. (a) Yaw rate and (b) side slip angle in a J-turn motion with 30% increased mass of the vehicle.

vehicle again look almost identical. Despite the parameter variations, the H_∞ controller still exhibits a good performance and stability.

In the third simulation, the yaw rate responses was measured with respect to different steering angle inputs for lane changes. Its results are shown in Figs. 10 and 11, where the trajectories of the uncontrolled vehicle become rather unstable, resulting in a large phase lag, as the amplitude of the steering angle becomes larger. On the other hand, the trajectories of the vehicle with the H_∞ controller remain very predictable and stay close to those of the model.

V. CONCLUSIONS

A model-based H_∞ controller which generates yaw moment by applying brake torque at one wheel at a time depending on the vehicle states in order to use the most efficient and consistently effective brake torque is designed. Its stability and performance robustness are assured by μ-analysis. The performance of the proposed controller is evaluated through a series of computer simulations based on a nonlinear tire model and a 8-DOF vehicle model. Simulation results show that the proposed controller exhibits robust stability and improved performance.

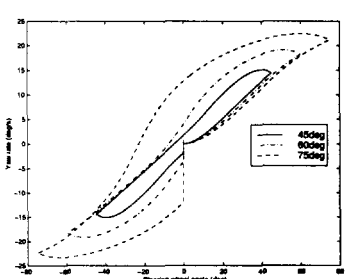

Fig. 10. Yaw rate responses in a uncontrolled vehicle.

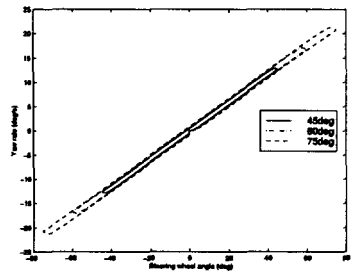

Fig. 11. Yaw rate responses in the H_∞-controlled vehicle.

REFERENCES

[1] M. Nagai, Y. Hirano, and S. Yamanaka, "Integrated control law of active rear wheel steering and direct yaw moment control," in *Proc. of AVEC*, pp. 451–469, 1996.

[2] M. Abe, N. Ohkubo, and Y. Kano, "A direct yaw moment control for improving limit performance of vehicle handling–comparison and cooperation with 4WS–," *Vehicle System Dynamics*, vol. 25, pp. 3–23, 1996.

[3] K. Koibuchi, M. Yamamoto, Y. Fukuda, and S. Inagaki, "Vehicle stability control in limit cornering by active brake," *SAE 960487*, 1996.

[4] S. Matsumoto, H. Yamaguchi, H. Inoue, and Y. Yasuno, "Improvement of vehicle dynamics through braking force distribution control," *SAE 920645*, 1992.

[5] A. Alleyne, "A comparison of alternative intervention strategies for unintended roadway departure (URD) control," *Proc. of AVEC*, pp. 485–506, 1996.

[6] A. van Zanten, R. Erhardt, and G. Pfaff, "VDC, the vehicle dynamics control system of Bosch," *SAE 950759*, 1995.

[7] H. Dugoff, P. S. Francher, and L. Segel, "An analysis of tire traction properties and their influence on the vehicle dynamic performance," *SAE 700377*, 1970.

[8] J. C. Doyle, K. Glover, P. P. Khargonekar, and B. A. Francis, "State-space solutions to H_2 and H_∞ control problems," *IEEE Trans. Automatic Control*, vol. 34, no. 8, pp. 831–847, 1989.

[9] K. Zhou, J. Doyle, and K. Glover, *Robust and Optimal Control*. Prentice Hall, 1996.